Photophysics of Nile Blue A in Proton-Accepting and Electron-Donating Solvents

Abderrazzak Douhal*

Institute for Molecular Science, Myodaiji, Okazaki 444, Japan

Received: June 16, 1994; In Final Form: October 1, 1994®

Nile Blue A perchlorate (NBA) dissolved in nonaqueous and hydrogen-bonding acceptor solvents (triethylamine and dimethylaniline) exhibits a ground-state intermolecular proton-transfer reaction. In weakly hydrogen-accepting solvents, the process is enhanced when the concentration of the dye is decreased. The reaction product, Nile Blue base, regenerates the parent molecule in the excited state via an intermolecular proton-transfer reaction with the solvent. Picosecond time-resolved fluorescence measurements suggest that the excited-state intermolecular proton-transfer process and the Stokes shift dynamics occur within 30 ps. In a weaker base and stronger electron-donor solvent, *N,N*-dimethylaniline, the fluorescence of NBA depends on the excitation wavelength. This is explained by a very efficient fluorescence quenching due to excited-state intermolecular electron transfer and by a reorganization of the solvation shell mainly caused by the excited-state intermolecular proton-transfer reaction.

I. Introduction

In recent years, the study of excited-state proton-transfer processes has become of great interest because of its chemical and biological relevance.[1] Prototropic effects in the ground and electronic excited states have been intensively investigated in a number of dyes and phenol derivatives.[1,2] Among the most thoroughly investigated systems are naphthol derivatives,[1,3] hydroxyleines,[4] 7-hydroxycoumarins,[5] tyrosine,[6] and 7-azaindole.[7] Other fluorescent dyes which show pH-dependent photophysics are fluorescein,[8] benzo[*c*]xanthene,[9−13] and oxazine derivatives.[14−16] The photochemistry and photophysics of these dyes involve important topics in physical chemistry, namely, (i) the effect the solvent has on the photophysical process, (ii) the surface crossing, in passing from an initially reached energy surface to another one, and (iii) the photoinduced proton- or electron-transfer reactions.

More specifically, the relative concentrations of the oxazine dye Nile Blue A perchlorate, NBA ($NBA^+ClO_4^-$), and its conjugate base, the neutral compound Nile Blue base (NBB) (Chart 1), in hydrogen-bonding solvents depend on the extent of the ground-state intermolecular proton-transfer reaction.[16−19] In fact, in the structure of the oxazine dyes, one can identify at least one group which can be very sensitive either to the basicity or to the acidity of the solvent. This would allow the formation of the conjugate base (or acid) in hydrogen-bonding solvents by an intermolecular proton-transfer reaction.

Recently, Kreller and Kamat[20] reported that cresyl violet (CV), another oxazine dye similar to NBA, shows changes in the absorption spectrum upon addition of amine that was ascribed to the formation of a charge-transfer complex, instead of the production of a proton-transfer reaction. However, other workers[14,21−24] have assigned these spectral changes of CV to hydrogen-bonding interactions with the solvent.

In the present work, we give spectroscopic evidence of ground- and excited-state intermolecular proton-transfer reactions of NBA, in electron-donating and proton-accepting (or hydrogen atom) solvents, like aniline derivatives. Our main reason to investigate the behavior of NBA in these solvents is

CHART 1

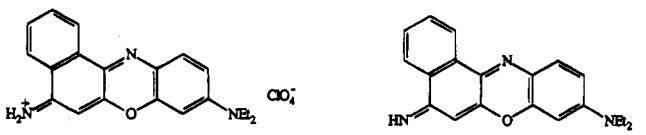

NBA NBB

because of the discovery of the ultrafast (ca. 100-fs) electron transfer from *N,N*-dimethylaniline (DMA) to electronically excited NBA,[25] producing a very efficient quenching of the dye fluorescence. The ultrafast rate of this process suggests that the electron transfer occurs without solvent fluctuation. The present work shows the excitation-wavelength dependence of the proton-coupled electron transfer of NBA in a hydrogen-accepting and electron-donating solvent such as *N,N*-dimethylaniline.

II. Experimental Section

Materials. Nile Blue A perchlorate (NBA) and oxazine 1 perchlorate (OX1) were obtained from Kodak and used without further purification. Nile Blue base (NBB) was synthesized from NBA.[17] 1-Chloronaphthalene (1CN) (analytical grade from Wako Pure Chemicals), triethylamine (TEA) (spectroscopic grade from Fluka), and acetonitrile (spectroscopic grade from Merck) were dried over silica gel before use. *N,N*-Dimethylaniline (DMA), from Katayama Chemicals, was vacuum distilled and stored under nitrogen before use.

Methods. Stationary absorption and fluorescence spectra were recorded with a Shimadzu (Model PC-310) spectrophotometer and a SPEX (Fluorolog 2) spectrofluorimeter, respectively. The optical density of the samples was kept below 0.2 au/cm at the excitation wavelength. Picosecond time-resolved fluorescence measurements were made with the time-correlated single-photon-counting method by using a synchronously-pumped mode-locked dye laser and a microchannel plate photomultiplier with an instrument response function of 40 ps FWHM.[26] Deconvolution of the fluorescence from the laser pulse allowed us to resolve decay (or rise) times of less than 10 ps. With rhodamine 6G as the laser dye, the excitation wavelength was tuned at 575 nm. The emission was collected at the "magic angle". The time-resolved fluorescence spectra

* Present address: Facultad de Químicas, Sección Campus de Toledo, Departamento de Química Física, c/ San Lucas 3, Universidad de Castilla-La Mancha, 45002 Toledo, Spain.

® Abstract published in *Advance ACS Abstracts,* November 15, 1994.

0022-3654/94/2098-13131$04.50/0

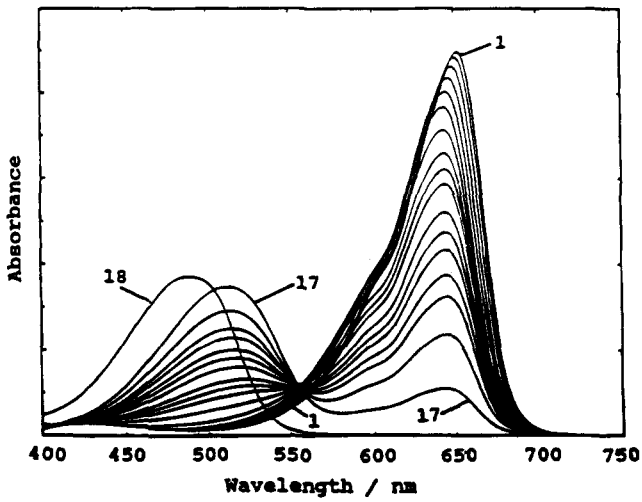

Figure 1. Variation of the absorption spectra of 2.7×10^{-5} M NBA in mixed solvents of 1CN and TEA. Spectra from the top (spectrum 1) to the bottom (spectrum 17) at the red side correspond to [TEA] = 0.0, 2.4, 3.6, 4.8, 6.0, 8.4, 10.8, 14.4, 17.9, 21.5, 24.1, 28.7, 39.5, 50.2, 71.8, 107, and 479×10^{-5} M, respectively. Spectrum 18 corresponds to 3.0×10^{-5} M NBB in neat TEA.

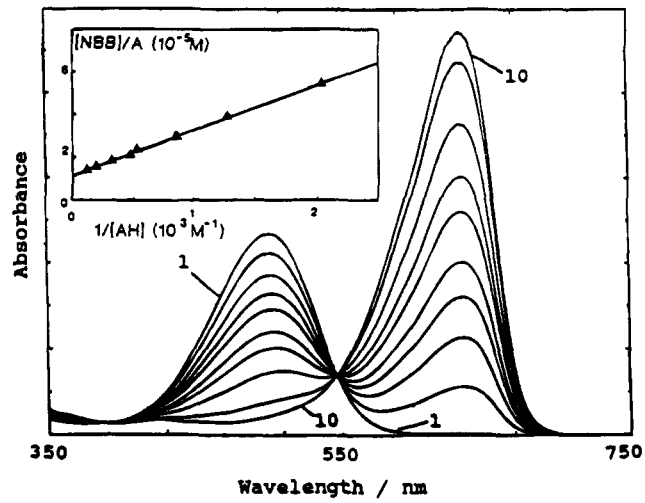

Figure 2. Variation of the absorption spectra of 3.5×10^{-5} M NBB in acetonitrile with the addition of acetic acid (AH). Spectra 1−10 correspond to [AH] = 0.0, 3.0, 5.0, 8.1, 11.9, 20.9, 23.8, 35.8, 62.4, and 107×10^{-4} M, respectively. The inset is a Benesi−Hildebrand plot at 630 nm. *A* is the absorption difference of NBB and NBA at 510 nm.

were constructed from fluorescence decays recorded at various emission wavelengths in 5-nm steps. The analysis of the fluorescence decay was done by a software package designed for simple and global analysis of fluorescence and anisotropy decay.[27] The decays and rise of fluorescence were obtained from the global analysis by linking them together and varying the preexponential factors at four emission wavelengths (600, 620, 650, and 700 nm). The quality of fit was estimated by the reduced χ^2, the distribution of the residuals, and the autocorrelation function.

III. Results and Discussion

A. Assignment of Ground-State Species. (1) Nile Blue A and Nile Blue B in Mixed Solvents. Figure 1 shows the absorption spectra of NBA (2.7×10^{-5} M) in mixtures of 1CN and TEA, which is a strong base. As 1CN has a similar polarity and a different ionization potential to those of aniline derivatives, it was chosen as a reference solvent in the electron-transfer process between NBA and these electron-donating solvents.[25] The figure also contains the absorption spectrum of NBB in pure TEA (spectrum 18). By comparing these spectra to that of NBB in TEA alone, one can assign the blue band at 510 nm to the absorption of NBB which is formed by the ground-state proton-transfer reaction between NBA and TEA. The deprotonation of NBA (or protonation of TEA) can be formulated as

$$NBA^+ + TEA \overset{K_1}{\rightleftharpoons} (NBB\text{-}H\text{-}TEA)^+ \overset{K_2}{\rightleftharpoons} NBB + TEAH^+ \quad (1)$$

where NBA^+ stands for $NBA^+ClO_4^-$ (NBA) and $TEAH^+$ for the protonated triethylamine.

The 21-nm blue shift of the absorption maximum of NBB in TEA, relative to that of NBB in the mixed solution of TEA and 1CN, is due to the large difference in polarity between pure TEA and the mixture TEA/1CN (1:1000). Thus, the polarity−polarizability (π^*) parameter values of TEA and 1CN are 0.14 and 0.71, respectively.[28] The most concentrated solution in TEA was 4.8×10^{-3} (spectrum 17), and therefore, the polarity of the medium was still governed by 1CN.

The absorption spectral features shown in Figure 1 suggest that the effect of TEA concentration can be divided in two regions: region I, where the concentration is low, [TEA] < 8×10^{-5} M (spectra 1−5); and region II for [TEA] higher than 8×10^{-5} M (spectra 6−17). In region I, the absorption in the blue side is weak, there are no isobestic points, and the formation of NBB is not evident. We cannot describe the change in absorption spectra by one equilibrium but rather by the involvement of three species as shown by eq 1. The first step in this equation is a prior formation of a complex between NBA and TEA via intermolecular H-bonding interaction. We do not exclude the existence of a small amount of NBB.

In region II, the formation of NBB by the proton-transfer reaction is more evident. There is a clear isobestic point. The system might be described by the second equilibrium of eq 1. The Benesi−Hildebrand (BH) plot,[29] the inverse of the absorption intensity at 510 nm as a function of the inverse of the concentration of TEA, is linear (not shown). From the slope and intercept of the plot, we obtained an equilibrium constant of 3300 M^{-1}, which corresponds to the second equilibrium of eq 1, and a molar absorption coefficient of NBB, $\epsilon_{510} = 26\,000$ M^{-1} cm^{-1}, which is comparable with that of NBB in neat TEA (25 000 M^{-1} cm^{-1}).

To elucidate the ground-state proton-transfer reaction, we further observed the absorption spectra of NBB in an acidified inert solvent, namely, mixtures of acetonitrile with acetic acid (Figure 2).

In this experiment, we started from the neutral form (NBB) in pure acetonitrile. The corresponding spectrum (number 1) shows a band at 503 nm and a molar absorption coefficient $\epsilon_{503} = 39\,000$ M^{-1} cm^{-1}. Upon addition of acetic acid, the intensity of this band decreases, creating a new absorption band in the red with a maximum at 632 nm (spectra 2 → 10). This process is the reverse of that taking place in NBA/1CN upon addition of TEA. The inset of Figure 2 shows the corresponding BH plot; the deduced equilibrium constant between NBA and NBB in these media and the molar absorption coefficient at 630 nm corresponding to NBA are 625 M^{-1} and 85 000 M^{-1} cm^{-1}, respectively. The molar absorption coefficient of NBA in 1CN is 51 000 M^{-1} cm^{-1}.[30] A previous study of NBA in mixtures of alcohols and acetic acid has shown the conversion of all the molecules to the acid form (NBA).[19]

(2) Nile Blue A/*N*,*N*-Dimethylaniline. The ground-state interactions between NBA and the solvent molecules were also

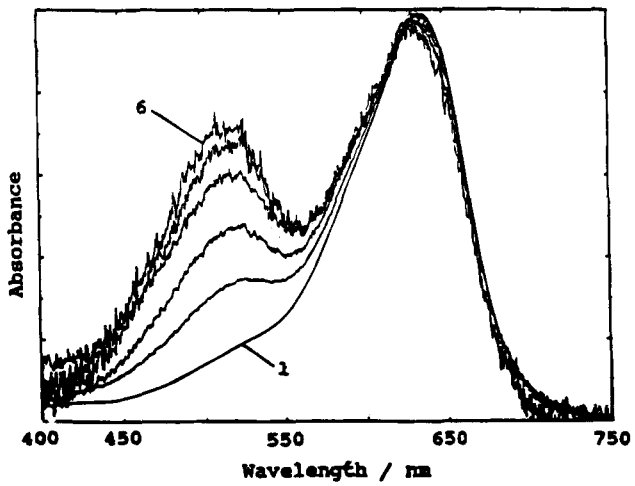

Figure 3. Normalized absorption spectra of NBA in neat DMA at [NBA] = 12.0, 3.5, 1.0, 0.7, 0.4, and 0.2 × 10^{-5} M from the bottom to the top at 510 nm.

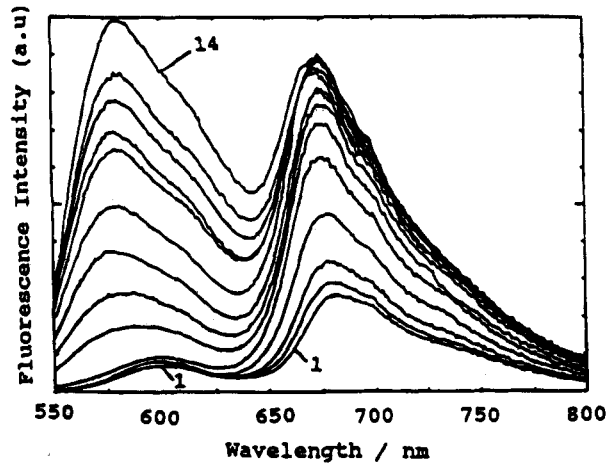

Figure 4. Steady-state fluorescence spectra of 2.7 × 10^{-5} M NBA in the mixture 1CN/TEA. Spectra 1−14 correspond to [TEA] = 0.0, 2.4, 3.6, 4.8, 6.0, 7.2, 8.4, 9.6, 10.8, 12.0, 14.4, 19.2, 24.0, and 28.7 × 10^{-5} M, respectively. The excitation wavelength was 510 nm.

investigated in neat DMA, which is a weakly hydrogen-bonding and strongly electron-donating solvent. DMA has an ionization potential of 7.12 eV compared with 7.50 eV for TEA.[31]

Figure 3 shows the absorption spectra of NBA in pure DMA at different concentrations of the dye. At [NBA] = 1.2 × 10^{-5} M, the absorption spectrum has its maximum at 628 nm and a shoulder around 505 nm. Dilution of this solution (spectra 1 → 6), with DMA, does not shift the principal band; however, it increases the relative intensity of the shoulder at 505 nm. In pure 1CN, we did not observe any change in this region of the absorption spectrum when we varied the concentration of NBA in the same range.

To explain the spectral changes shown in Figure 3, we recall the result of Figure 1 (the formation of NBB due to a ground-state intermolecular proton-transfer reaction between NBA and a base) and the general increase in the molar fraction of dissociation of weak acids upon dilution. Thus, the band at 505 nm results from the absorption of the neutral form, NBB, formed by a proton-transfer reaction between NBA and DMA.

Oxazine 1, with two diethyl amino groups (NBA has one amino group and one diethyl amino group), has a comparable structure to that of NBA. It does not display the phenomenon exhibited by NBA in the ground state; i.e., the absorption spectrum does not change with the concentration of dye either in neat 1CN or in neat DMA. The experiment with oxazine 1 is also consistent with the mechanism of proton transfer in the ground state for a dilute solution of the NBA/DMA system.

As we noted in the Introduction, Kreller and Kamat reported the absorption spectra of CV (which has two amino groups in the oxazine skeleton) in mixtures of methanol and amines.[20] They assigned the blue absorption band, which appears when the solution is rich in amine, to a charge-transfer complex between CV and amine. However, in more than one study, hydrogen bonding between CV and solvent is suggested to explain the chemical and photophysical behavior of CV.[14,21-24] Our experimental result indicates that the process involves a ground-state hydrogen-bonding interaction and the formation of the conjugate base absorbing in the blue side of the spectrum. A similar result showing the coexistence of neutral (NBB) and cationic (NBA) forms in neat alcohols has recently been reported.[18]

B. Excited-State Intermolecular Proton Transfer. (1) Nile Blue A in the Mixed Solvents of 1CN/TEA. Figure 4 shows the steady-state fluorescence spectra of NBA in the mixtures of 1CN and TEA, with excitation at 510 nm. Before discussion

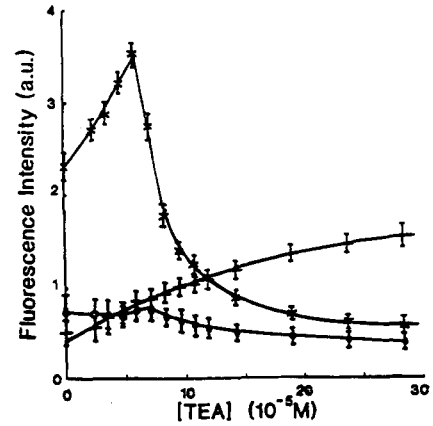

Figure 5. Variation of the normalized fluorescence intensity of NBA (2.7 × 10^{-5} M) in 1CN with concentration of TEA. Excitation wavelengths: 510 nm (*), 590 nm (+) and emission wavelength: 700 nm. Excitation wavelength: 510 nm and emission wavelength: 600 nm (○).

of these spectra, we assign the blue band to the fluorescence of NBB (λ_{max} = 580 nm) and the red one to NBA (λ_{max} = 675 nm). Excitation of these solutions at 590 nm leads to the fluorescence of NBA at 675 nm (spectra not shown).

Figure 5 shows a plot of the fluorescence intensity of NBA at 700 nm when the concentration of TEA is increased and when we excited it at two different regions (510 and 590 nm) of the absorption spectrum. The data in Figure 5 have not been corrected by the relatively small contribution to the total absorption at 510 and 590 nm of the concentration changes of NBA and NBB, respectively, upon addition of TEA. We recall that at 510 nm, the absorption is mainly due to NBB, and at 590 nm, the absorption is mainly due to NBA. The emission at 700 nm is due to excited NBA.

Figure 5 shows a linear increase of the fluorescence intensity of NBA at 700 nm in these mixtures when we excited it at 590 nm (spectra not shown). At [TEA] = 1.4 × 10^{-4} M, the change of the fluorescence intensity deviates from linearity. Notice that upon addition of TEA, the absorption spectrum of NBA shifts by 5 nm to the blue, which is due to the establishment of a hydrogen bond with TEA (Figure 1 and eq 1). The increase of the fluorescence intensity of NBA at the 675-nm band when TEA was added can be explained by a decrease of the nonradiative rates due to the establishment of a hydrogen bond with TEA. Hydrogen-bonded (and ionized) rhodamine B (via CO_2H) is more fluorescent than the ones without,[12] and

protonated benzo[c]xanthene is also more fluorescent than the neutral one.[13]

The increase in the fluorescence intensity of NBA follows the TEA concentration when we excited it at 590 nm; this is not the case when it is excited at 510 nm (Figure 5). For a concentration of TEA lower than 6×10^{-5} M (region I), the fluorescence intensity exhibits a linear increase and shows a plot different from that when we excited it at 590 nm. This behavior is just another way to observe the prior establishment of an intermolecular hydrogen bond between NBA and TEA prior to full proton transfer. Under these conditions (λ_{exc} = 510 nm and [TEA] $< 6 \times 10^{-5}$ M), the excited species is a "hydrogen-bonded complex" of NBB and protonated TEA. The increase of fluorescence intensity at 700 nm can be explained by the formation of NBA in the excited state due to the reverse intermolecular proton-transfer reaction. However, the NBB fluorescence intensity does not show any decrease due to this process. Assuming that the most efficient ways to depopulate the excited $(NBB{\cdots}H{\cdots}TEA)^+$ species are (i) the reverse excited-state intermolecular proton transfer (k_{PT}) to produce excited NBA and (ii) radiative (k_r) and (iii) nonradiative (k_{nr}) transitions to its ground state, a possible explanation for the behavior of NBB fluorescence in these [TEA] conditions would be the compensation of the k_{PT} increase with a decrease in k_{nr}, both produced by the change of the medium on the TEA addition.

For [TEA] higher than 6×10^{-5} M (region II) and excitation at 510 nm, the fluorescence intensity of NBA decreases when adding TEA. This might be the result of the existence of a nonfavorable solvation shell of NBB in the ground state which prevents the formation of NBA in the excited state. When the concentration of TEA is high, the solvation of NBB (other than hydrogen bonding) by surrounding TEA molecules in the excited state may weaken the hydrogen-bonding interaction between protonated TEA and NBB. The reverse proton transfer in the excited state seems to be affected by the concentration of TEA.

The plot of the absorbance-corrected fluorescence intensity at 600 nm when the excitation wavelength was 510 nm shows a small decrease of the fluorescence intensity of NBB when increasing the concentration of TEA (Figure 5). This seems to be not in accordance with the decrease of NBA fluorescence intensity due to the nonfavorable solvation shell of NBB, which prevents the occurrence of the excited-state proton-transfer reaction. One plausible explanation would be that at much higher [TEA] concentration, the k_{nr} of NBB in this solvation shell increases with [TEA], leading to a fluorescence quenching of NBB.

Proton transfer appears to be predominantly responsible for the formation of NBB in the ground state, which is also the case for the formation of NBA in the excited state. Hydrogen-bonding interactions can play an important role in the photophysics of NBA as well as any process that may contribute to an increase in its nonradiative decay rate.

We note that even in the absence of TEA, NBA in 1CN exhibits a fluorescent band at 600 nm which we attribute to a small amount of NBB formed by reaction between NBA and water contained in 1CN. The intensity of this band decreased when a sufficiently dried 1CN over a silica gel was used.

In Figure 6, we report a picosecond time-resolved fluorescence decay of a dilute solution of NBA (3×10^{-5} M) in a mixture of 1CN and TEA (1.5×10^{-4} M) at 600 and 700 nm. The excitation wavelength was 575 nm. At this TEA concentration, the solution may consist of three species of NBB, NBA, and the "complex" $(NBB{\cdots}H{\cdots}TEA)^+$. The global analysis of the decays measured at 600−700 nm permits the linking of lifetimes (in this case, three different lifetimes in four decays)

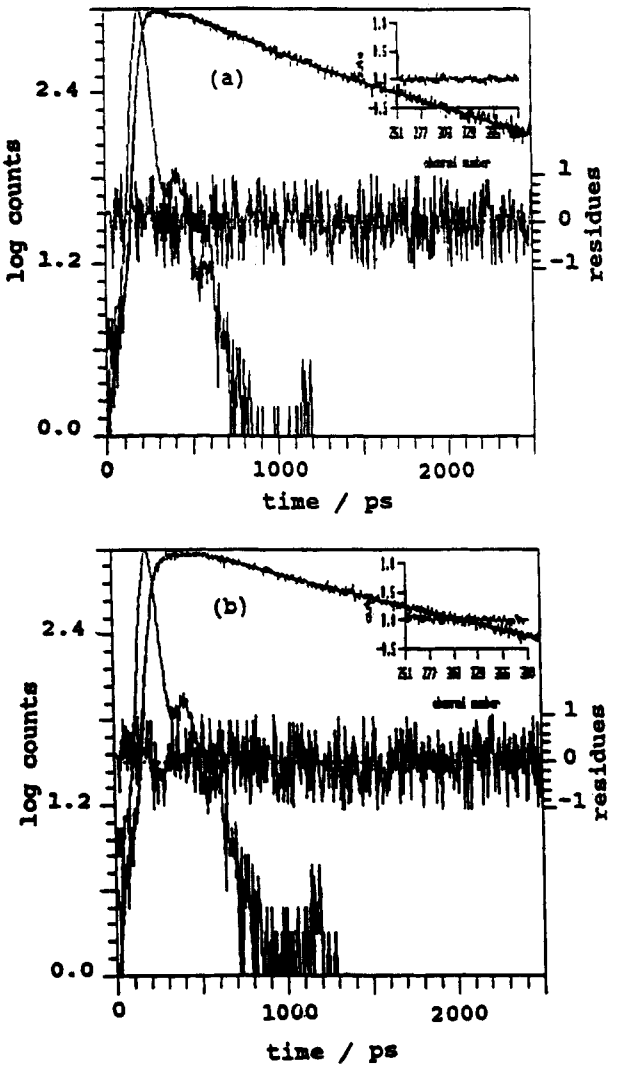

Figure 6. Time-resolved fluorescence decay of 3.0×10^{-5} M NBA in mixed solvents of 1CN and TEA (1.5×10^{-4} M) (upper curves). The excitation wavelength was 575 nm; the emission wavelengths were 600 (a) and 700 nm (b). Also shown is the laser pulse shape (lower curves) obtained by the scatter light through the detection system; 1 channel corresponds to 4.88 ps. The insets in a and b are the autocorrelation functions of the residues. The fitting parameters are (a) $a_1 = 0.6$, $t_1 = 1.54$ ns, $a_2 = 0.6$, $t_2 = 0.41$ ns, $a_3 = 0.2$, $t_3 = 30$ ps, $\chi^2 = 1.02$. (b) $a_1 = 0.9$, $t_1 = 1.54$ ns, $a_2 = 0.3$, $t_2 = 0.41$ ns, $a_3 = -0.9$, $t_3 = 30$ ps, $\chi^2 = 0.96$. a_i and t_i are the preexponential factor and the fluorescence lifetime, respectively.

observed at different wavelengths. The best fit gives a global χ^2 of 1.03. The result from this analysis shows that the fluorescence at different wavelengths of the emission spectrum leads to two decays of 0.41 and 1.54 ns and a rise of 30 ps at longer wavelengths (650−700 nm). The 30-ps component becomes a decay at short emission wavelengths. The subnanosecond component (0.41 ns) does not contribute much in the decay at the red side of the emission spectrum (greater than 650 nm). Therefore, we attribute this lifetime to that of excited NBB and 1.45 ns to NBA. The 30-ps decay at shorter emission wavelengths and rise at longer ones suggests the production of (i) a picosecond Stokes shift dynamics (spectral relaxation) and/or (ii) an excited-state reaction in NBB/protonated solvent leading to the formation of fluorescent species (NBA) in the red region of the emission spectrum in accordance with the results of Figure 4.

Figure 7 shows time-resolved emission spectra in the same experimental conditions. These spectra show a clear spectral shift at the red band. The blue part of these spectra is affected

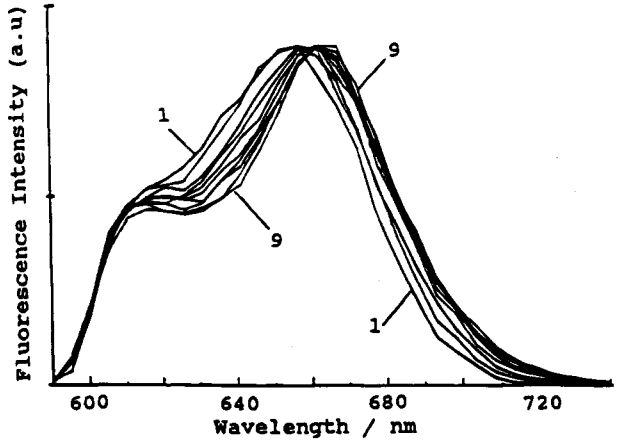

Figure 7. Normalized picosecond time-resolved fluorescence spectra of 3.0×10^{-5} M NBA in the mixture 1CN/TEA: [TEA] = 1.5×10^{-4} M. The gating times from spectrum 1 to 9 are respectively 25, 49, 73, 98, 122, 171, 293, 488, and 683 ps. The observed window is 15 ps for every spectrum.

by the cut-off filter (600 nm) used before the detection system for the purpose of avoiding scattered light from laser excitation (575 nm).

The dynamics of the Stokes shift are quantified by measuring the correlation function, $C(t)$, defined by

$$C(t) = [\nu(t) - \nu(0)]/[\nu(\infty) - \nu(0)] \qquad (2)$$

where $\nu(0)$, $\nu(t)$, and $\nu(\infty)$ are the wavenumbers of the emission maxima at times zero, t, and infinity (fully relaxed).[32] Attempts to calculate this Stokes shift correlation function for NBA emission were hindered by the small overall shift of the fluorescence spectrum of NBA ($\approx$10 nm) and the overlap between this spectrum and that of NBB. The Stokes shift dynamics in the system NBA/1CN has been observed to occur with the approximate experimental decay of 18 ps.[30] Also, the fluorescence dynamics of NBA in methanol resulted in a two-exponential wavelength shift of the maximum with a fast component along with a 20-ps component.[33] The slow component was assigned to solvation dynamics. A time-resolved study of NBA in ethanol reported by Martin et al. showed that the red shift of the transient gain spectra is completed within 20 ps after subpicosecond excitation of the sample.[34] Therefore, the picosecond component (30 ps) of the fluorescence decays of NBA in a mixture of 1CN and TEA can be assigned to (i) the time of the reverse proton-transfer reaction in the excited state which generates NBA after an excited-state intermolecular proton transfer in the H-bonded complex $(NBB{\cdots}H{\cdots}TEA)^+$ and (ii) Stokes shift dynamics.

(2) Nile Blue A in Neat DMA. After establishing some photochemical and photophysical processes of NBA in the presence of a strong H-accepting solvent, we will now study its behavior in the presence of a solvent which has both an electron-donating and weakly hydrogen-accepting nature. The solvent used in this case is DMA.

We recorded the fluorescence spectra of a dilute solution of NBA in DMA; i.e., [NBA] = 1.2×10^{-5} M. Excitation at 490 nm leads to a fluorescence spectrum with two fluorescence bands with maxima at 578 and 685 nm (Figure 8). However, excitation at 590 nm gives a very weak fluorescence (not shown). We note that the maximum of emission of NBA in 1CN is at 675 nm (Figure 4). At a higher concentration of the dye, the emission at 578 nm is affected by autoabsorption in this region.

Comparing the spectra of Figure 8 and those of Figure 4 suggests that the blue emission band (578 nm) is due to NBB

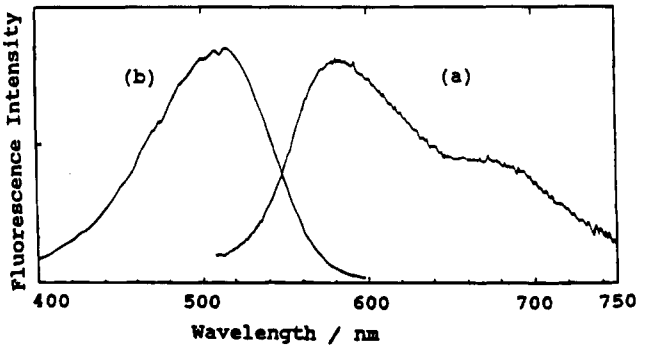

Figure 8. Steady-state (a) fluorescence and (b) excitation spectra of 1.2×10^{-5} M NBA in DMA for (a) λ_{exc} = 490 nm and (b) λ_{em} = 580 or 720 nm.

(as in TEA) and the red emission band (685 nm) is due to NBA as in 1CN (675 nm). Taking into account that the absorption maxima of NBA in DMA are at 628 nm and in 1CN are at 650 nm, we suggest that the large Stokes shift in DMA is due to the stronger interaction between NBA and this solvent. This interaction can lead to a fast intermolecular electron-transfer reaction when the configuration NBA−DMA is favorable to this process.

The red fluorescence (685 nm) upon excitation of the solution at 490 nm suggests the formation of NBA in the excited state. After photonic excitation of NBB (which absorbs around 510 nm), solvent relaxation leads one of the protonated solvent molecules ($DMAH^+$) to give a proton to NBB by an excited-state intermolecular proton-transfer reaction. Examination of the pK_a upon electronic excitation of NBB (pK_a = 4.3,[19] pK^*_a = 11.3[35]) and protonated DMA ($DMAH^+$, pK_a = 5.1[36]) agrees with a possible production of an excited-state intermolecular proton transfer from $DMAH^+$ to NBB. Thus, on electronic excitation, NBB becomes basic (pK^*_a = 11.3) enough to be able to partially recover a proton from $DMAH^+$, if not fully. The yield of protonation of NBB depends on the structure of its solvation shell, the excited-state proton-transfer dynamics, and the energy barrier of the excited potential energy surfaces of NBB and NBA. The fluorescence excitation spectrum is both independent of the emission wavelength and different from the total absorption spectrum (Figure 8). Hence, both fluorescence bands at 578 and 685 nm originate from two species having a common ground-state species ($NBB{\cdots}DMAH^+$) (chart 1 in Figure 9).

To explain the "strong" fluorescence (685 nm) due to NBA in DMA as a result of excited-state intermolecular proton-transfer reaction, one has to consider two possible structures of the solvation shell of NBA/DMA: (i) a shell with very weak or no specific (H-bonding) interactions between NBA and the molecules of DMA; (ii) a shell where a solvent molecule has either established a strong NBA−DMA H-bond or removed a proton from the dye in the ground state ($NBB{\cdots}DMAH^+$). Electronic excitation of this solvated H-bonded complex (shell ii, chart 1 in Figure 9) leads to a proton-transfer reaction producing excited NBA in a solvation shell different from that of shell i where NBA is simply solvated by molecules of DMA (chart 2 in Figure 9). It is worth noting that excitation of shell i leads to an ultrafast intermolecular electron-transfer reaction from DMA to NBA, resulting in a severe fluorescence quenching of NBA.[25] Therefore, *the most favorable solvation shell for an excited-state intermolecular proton transfer is different from the ones for an excited-state intermolecular electron-transfer reaction.* The formed NBA in the excited-state proton-transfer process has a solvation shell nonfavorable for an ultrafast quenching of fluorescence by electron transfer. The

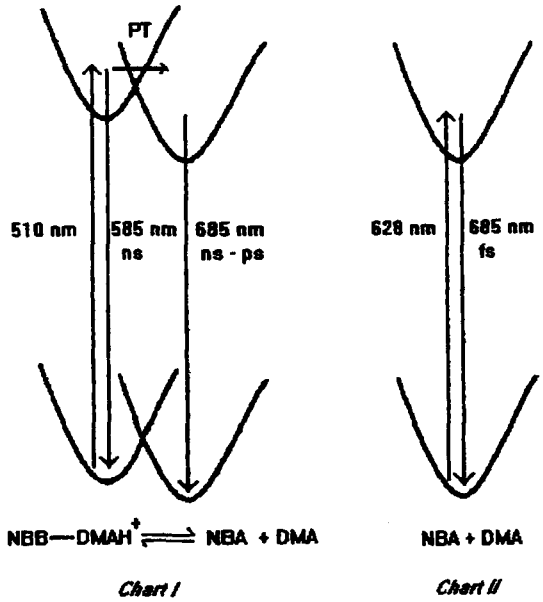

Figure 9. Schematic diagram of the potential energy surfaces of NBA in DMA.

system might need some time to reorganize the surrounding medium for the occurrence of this reaction (Figure 9). More than 3 decades ago, Mataga suggested the charge-transfer interaction between proton−donor and −acceptor π-electron systems via the hydrogen bond as a possible mechanism of the fluorescence quenching.[37] Recent femtosecond laser photolysis studies on the mechanisms of photoinduced electron transfer in 1-aminopyrene−pyridine H-bonded complexes have shown that the process is greatly assisted energetically by specific H-bonding interactions and also dynamically by a little movement of the protont from the H-donor to the H-acceptor in the formed H-bond.[38] On the other hand, the proton-coupled electron transfer is a well-elaborated theme in the study of biological assembly.[39]

Regarding the existence of two structures of shells of NBA in DMA, more interestingly shell ii (chart 1 in Figure 9), one can expect a multicomponent decay of the fluorescence of NBA in DMA following the evolution of the solvation shell of the H-bonded complex NBA···DMA (or NBB···DMAH$^+$) in the potential energy surfaces. This last situation reflects the case of a "wide reaction window" in the Marcus theory, where the solvent plays a role in the electron-transfer dynamics.[40] In this case, the electronic matrix element, responsible for the electron transfer, depends on the proton-solvation-shell configuration which will dictate the fluorescence dynamics. A multiexponential behavior of excited NBA in DMA is expected. This prediction is in agreement with the biexponential decay of NBA in DMA (or aniline)[25] and the nature of the decays of OX1 in DMA (single exponential) and in aniline (biexponential).[41] As we noted previously, OX1 cannot establish a H-bond with DMA, and consequently, a proton-coupled electron-transfer mechanism is not possible. This last process ascribes the "narrow reaction window" case in the Marcus theory, where the solvent does not move for the cause of the process.[40] The quenching of fluorescence of OX1 in DMA is due to a fast electron transfer, and the process does not depend on the excitation and emission wavelengths.[41] In the case of NBA "solvated" in shell i (with a very weak or a lack of H-bond with DMA), the occurrence of electron transfer may not require any proton dynamics.

Further work is needed and is in progress to elucidate the competition between excited-state electron transfer, H-bonding interaction, and the nature of multiexponential fluorescence decays of oxazine derivatives in proton-accepting and electron-donating solvents.[42] Very recently, a theoretical treatment of the mechanism for proton-coupled electron transfer has been reported and predicts the dependence of the electron-transfer rate on the proton configuration and dynamics.[43]

IV. Conclusions

In this work, we have shown that the ground-state interaction of NBA with proton-accepting solvents leads to the formation of the conjugate base NBB. The process involves an intermolecular proton-transfer reaction. We showed that this ground-state interaction also depends on the nature of the solvent and the concentration of the dye. Picosecond time-resolved fluorescence measurements of NBA in a mixture of 1CN and TEA suggest that the excited-state proton transfer and the dynamics of Stokes shift occur within 30 ps. The fluorescence of NBA in neat DMA depends on the excitation wavelength. When NBA is produced in the excited state by an intermolecular proton transfer, the fluorescence is stronger than that of NBA produced by a simple vertical electronic transition leading to a fast electron-transfer reaction. It is suggested that the solvation shell created by the proton-transfer reaction affects the rate of the excited-state intermolecular electron-transfer process. This gives experimental evidence on the dependence of electron-transfer mechanisms on the proton configuration and dynamics of the oxazine family in aniline derivatives.

Acknowledgment. The advice and interest in this work from Prof. K. Yoshihara are most gratefully acknowledged; thanks also to Prof. A. U. Acuña and to Dr. M. Martin for reading and criticizing the manuscript. Financial support from the Japanese Ministry of Education, Science, and Culture and the Japanese Society for the Promotion of Science is also very appreciated. This work is dedicated to my daughter, Yasmín, for her first birthday.

References and Notes

(1) (a) Special Issue of *Chem. Phys.* **1989**, 136. (b) Special Issue of *J. Phys. Chem.* **1991**, 95. (c) Arnaut, L.; Formosinho, S. J. *J. Photochem. Photobiol. A: Chem.* **1993**, *75*, 1. Formosinho, S. J.; Arnaut, L. *J. Photochem. Photobiol. A: Chem.* **1993**, *75*, 21.

(2) Ireland, J. F.; Wyatt, P. A. H. *Adv. Phys. Org. Chem.* **1972**, *12*, 131−221.

(3) Vander Donckt, E. *Prog. React. Kinet.* **1970**, *5*, 274−299.

(4) (a) Haylock, J. C.; Mason, S. F.; Smith, B. E. *J. Chem. Soc.* **1963**, 4898. (b) Douhal, A.; Sastre, R. *Chem. Phys. Lett.* **1994**, *91*, 219. Lahmani, F.; Douhal, A.; Breheret, E.; Zenhacker-Retien, A. *Chem. Phys. Lett.* **1994**, *235*, 220 and references therein.

(5) Huber, J. R.; Nakashima, M.; Sousa, J. A. *J. Phys. Chem.* **1973**, *77*, 860.

(6) Rayner, D. M.; Krajcarski, D. T.; Szabo, A. G. *Can. J. Chem.* **1978**, *56*, 1238.

(7) Taylor, C. A.; El-Bayoumi, M. A.; Kasha, M. *Proc. Natl. Acad. Sci. U.S.A.* **1969**, *63*, 253.

(8) (a) Thomas, J. A.; Buchsbaum, R. N.; Zimniak, A.; Racker, E. *Biochemistry* **1979**, *18*, 2210. (b) Martin, M. M.; Linqvist, L. *J. Luminesc.* **1975**, *10*, 381.

(9) Whitaker, J. E.; Haugland, R. P.; Prendergast, F. G. *Anal. Biochem.* **1991**, *194*, 330.

(10) Ferguson, J.; Mau, A. W. H. *Chem. Phys. Lett.* **1972**, *17*, 543.

(11) Ferguson, J.; Mau, A. W. H. *Aust. J. Chem.* **1973**, *26*, 1617.

(12) Sadkowski, P. J.; Fleming, G. H. *Chem. Phys. Lett.* **1978**, *57*, 526.

(13) Martin, M. M. *Chem. Phys. Lett.* **1975**, *35*, 105; **1976**, *43*, 332.

(14) Drexhage, K. H. In *Dye Lasers*; Schaefer, F. P., Ed.; Springer-Verlag: New York, 1977; Chapter 4.

(15) Gvishi, R.; Resfeld, R. *Chem. Phys. Lett.* **1989**, *156*, 181 and references therein.

(16) (a) Stuzka, V.; Hanus, V. *Acta Univ. Palack. Olumuc. Rac. Rerum. Natur. Chem.* **1978**, *57*, 121. (b) Goryaeva, E. M.; Shablya, A. V. *Zh. Prikl. Spectrosk.* **1985**, *43*, 750.

(17) Dutt, G. B.; Doraiswamy, S. *J. Chem. Phys.* **1992**, *96*, 2475.

(18) Williams, A. D.; Jiang, Y.; Ben-Amotz. D. *Chem. Phys.* **1994**, *180*, 119.

(19) Davis, M. M.; Hetzer, H. B. *Anal. Chem.* **1966**, *38*, 451.

(20) Kreller, D. I.; Kamat, P. V. *J. Phys. Chem.* **1991**, *95*, 4406.

(21) Guiliani, J. F.; Barrett, T. W. *Spectrosc. Lett.* **1985**, *16*, 750.

(22) Ghigalova, E. B.; Morozova, Y. P.; Russ, J. *J. Phys. Chem.* **1985**, *59*, 1010.
(23) Nizamov, N.; Umarov, K. U.; Dzhumadinov, R. K.; Atakhodzhaev, A. K. *Opt. Spectrosc.* **1983**, *54*, 600.
(24) Isak, S. J.; Eyring, E. M. *J. Photochem. Photobiol. A: Chem.* **1992**, *64*, 343.
(25) Kobayashi, T.; Takagi, Y.; Kandori, H.; Kemnitz, K.; Yoshihara, K. *Chem. Phys. Lett.* **1991**, *180*, 416.
(26) Yamazaki, I.; Tamai, N.; Kume, H.; Tsuchiya, H.; Oba, K. *Rev. Sci. Instrum.* **1985**, *56*, 1187.
(27) Beechem, J. M.; Gratton, E.; Mantulin, W. *Globals Unlimited*; University of Illinois: Chicago, 1990.
(28) Kamlet, M. J.; Doherty, R. M.; Abrams, M. H.; Marcus, Y.; Taft, R. *J. Phys. Chem.* **1988**, *92*, 5244.
(29) Benesi, H. A.; Hildebrand, J. H. *J. Am. Chem. Soc.* **1949**, *71*, 2703.
(30) Kandori, H.; Kemnitz, K.; Yoshihara, K. *J. Phys. Chem.* **1992**, *96*, 8042.
(31) Nagy, O. B.; Dupire, S.; Nagy, J. B. *Tetrahedron* **1975**, *31*, 2453.
(32) Bagchi, D.; Oxtoby, D. W.; Fleming, G. R. *Chem. Phys.* **1984**, *86*, 257.
(33) Mokhtari, A.; Chesnoy, J.; Laubereau, A. *Chem. Phys. Lett.* **1989**, *155*, 593.
(34) Martin, M. M.; Hung, N. D.; Picard, L.; Plaza, P.; Meyer, M. In *Ultrafast Processes in Spectroscopy*; Lauberreau, A., Seilmeier, A., Eds.; Inst. Phys. Conf. Ser. 126; IOP: Beyrouth, Germany, 1992; p 519.
(35) The pK^*_a value was calculated by the cycle of Forster: $pK^*_a = pK_a - (0.629/T)(u_n - u_p)$, where u_n and u_p are the energies (in cm^{-1}) of the 0−0 transition in the neutral and protonated forms, respectively. The 0−0 transitions were taken to be the average energies of the absorption and emission maxima for the two forms.
(36) Bridges, J. W.; Williams, R. T. *Biochem. J.* **1968**, *107*, 225.
(37) (a) Mataga, N.; Tsuno, S. *Naturwissenschaften* **1956**, *10*, 305. (b) Mataga, N.; Tsuno, S. *Bull. Chem. Soc. Jpn.* **1957**, *30*, 711. (c) Mataga, N. *Ibid.* **1958**, *31*, 481. (d) Mataga, N.; Torihashi, Y.; Kaifu, Y. *Z. Phys. Chem. (Frankfurt/Main)* **1962**, *34*, 379.
(38) Miyasaka, H.; Tabata, A.; Kamada, K.; Mataga, N. *J. Am. Chem. Soc.* **1993**, *7335*, 115.
(39) See, for example: Kirmayer, C.; Holten, D. In *The Photosynthetic Bacterial Reaction Center—Structure and Dynamics*; Breton, J., Vermeglio, A., Eds.; Plenum: New York, 1988; p 219.
(40) Sumi, H.; Marcus, R. A. *J. Chem. Phys.* **1986**, *84*, 4894.
(41) (a) Yoshihara, K.; Yartsev, A.; Nagasawa, Y.; Kandori, H.; Douhal, A.; Kemnitz, K. *Pure Appl. Chem.* **1993**, *65*, 1671. (b) Yartsev, A.; Nagasawa, Y.; Douhal, A.; Yoshihara, K. *Chem. Phys. Lett.* **1993**, *207*, 546. (c) Yoshihara, K.; Yartzev, A.; Nagasawa, Y.; Kandori, H.; Douhal, A.; Kemnitz, A. In *Ultrafast Phenomena*; Martin, J.-L., Migus, A., Mourou, G. A., Zewail, A. H., Eds.; Springer-Verlag: Berlin Heidelberg, 1993; Vol. VIII, p 571.
(42) Douhal, A.; Yoshihara, K. To be published.
(43) Cikier, R. I. *J. Phys. Chem.* **1994**, *98*, 2377.